This is a repository copy of *Efflorescence and subflorescence induced microstructural and mechanical evolution in fly ash-based geopolymers*.

Efflorescence and subflorescence induced microstructural and mechanical evolution in fly ash-based geopolymers

Zuhua Zhang [1, 2]*, John L. Provis [3], Xue Ma [4], Andrew Reid [5], Hao Wang [1]*

1. Centre for Future Materials, University of Southern Queensland, Toowoomba, Queensland 4350, Australia.

2. Key Laboratory for Green & Advanced Civil Engineering Materials and Application Technology of Hunan Province, College of Civil Engineering, Hunan University, Changsha 410082, PR China.

3. Department of Materials Science and Engineering, The University of Sheffield, Sheffield S1 3JD, United Kingdom.

4. School of Materials Science and Engineering, Southwest University of Science and Technology, Mianyang 621010, China.

5. Halok Engineering Pty Ltd. Level 1, 162 Boundary Street, West End QLD 4101, Australia.

*Corresponding author: Zuhua.Zhang@usq.edu.au; Hao.Wang@usq.edu.au

Abstract

This paper reports the effects of efflorescence on the microstructural and mechanical properties of fly ash-based geopolymers. Geopolymer pastes manufactured by sodium hydroxide and sodium silicate activation of three Class F fly ashes exhibit varying efflorescence behaviour. The geopolymer derived from sodium silicate activation of fine fly ash, which has a compact microstructure, shows a relatively slow efflorescence rate and low efflorescence potential. The efflorescence occurring on the surface of the geopolymer specimens does not change their mineralogical characteristics. However, the compressive strength development and compressive modulus of geopolymers can be affected through processes related to the loss of alkalis, and also to subflorescence. The phenomenon of subflorescence can be regarded as an extended efflorescence taking place under the surface of the material, leading to crystallisation pressure, which may exceed the tensile strength of hardened binders and generate structural damage.
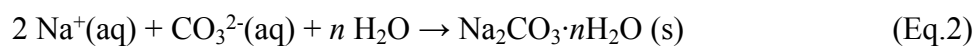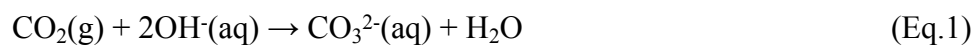
1. Introduction

Efflorescence is frequently encountered on the surface of Portland cement (PC) based masonry and concrete constructions. The underlying mechanisms for efflorescence of these materials involve a set of physiochemical processes which lead to deposition of white salts on the exterior of the materials. The primary chemical reaction is a superficial carbonation process that involves the dissolution and diffusion of Ca^{2+}, dissolution of atmospheric CO_2 in the surface liquid, and precipitation of calcium carbonate ($CaCO_3$) during drying. The release of alkalis and other salts from cement components or aggregates, and the transport of salts (e.g. alkalis and sulfates) from the ground through concrete to a drying surface, can promote and lead to efflorescence, even though these salts do not necessarily form part of the solid $CaCO_3$ efflorescence deposit [1,2]. To avoid and mitigate efflorescence, which is normally structurally harmless but aesthetically undesirable, the first recommended step is to reduce the alkali concentration of the cements so as to reduce the solubility and absorption rate of CO_2 from the ambient environment [2].

A different efflorescence situation has arisen due to the development of geopolymer cement and concrete in the last decades. Geopolymer cement is manufactured by alkali activation of solid aluminosilicate precursors at ambient or slightly elevated temperature conditions, in the presence of little or no available calcium. The most widely used aluminosilicate precursors are calcined clay (usually metakaolin), fly ash, or their blends. The alkali activator can be a concentrated alkali hydroxide or alkali silicate solution, such as NaOH or Na_2SiO_3, which provides the high-pH conditions required to initiate the geopolymerisation reaction. The amount of liquid required for geopolymer mixing depends strongly on the type and the properties of the solid precursor: metakaolin-based geopolymer pastes usually require a

liquid/solid mass ratio (L/S) higher than 0.6 to achieve suitable workability for casting [3, 4] and the corresponding mortars need L/S around 1.0 [5, 6]. Depending on the properties of the fly ash selected (especially particle size and distribution) and the required workability, fly ash-based geopolymer pastes usually require L/S ~ 0.30-0.65 [7] and the concretes need L/S of 0.40–0.96 [8]. Regardless of the amounts of liquid used for mixing, the normal alkali content required in fly ash based geopolymer binders to obtain useful strength, and strength development rate, for construction purposes is 3-10% (expressed as a mass ratio of Na_2O to the solid precursor) [7-9]. Such an alkali content is 10 to 20 times higher than is common in Portland cement. This leads to concerns regarding efflorescence, as observations of many geopolymer mixes did find efflorescence that rapidly occurred on drying surface when samples are in contact with water [10-14].

Our previous study [15] investigated the relationship between composition, pore structure and efflorescence in fly ash-based geopolymers, and highlighted that the efflorescence reactions are distinct from those which occur in PC based materials, resulting in an alkali carbonate solid deposit rather than the calcium carbonates observed in PC, eqs. 1-2:

$$CO_2(g) + 2OH^-(aq) \rightarrow CO_3^{2-}(aq) + H_2O \qquad\qquad (Eq.1)$$

$$2\ Na^+(aq) + CO_3^{2-}(aq) + n\ H_2O \rightarrow Na_2CO_3 \cdot nH_2O\ (s) \qquad\qquad (Eq.2)$$

The availability of OH^- and Na^+ is critical for this process to lead to the deposition of sodium carbonate hydrates; high alkalinity accelerates the uptake of CO_2 into an aqueous environment [2], while the sodium is required for crystalline salt deposition, which is much less evident if the alkali used in producing the geopolymer is potassium. Although hydrothermal curing and addition of blast furnace slag (or another source of reactive calcium) can reduce the efflorescence rate, they appear to have very limited effects on the overall efflorescence potential, as indicated by the pH and the leaching extents of sodium from solid

specimens [15]. Given the high alkalinity of geopolymer cement and the high mobility of alkalis (especially for the sodium based binders), efflorescence is an intrinsic behaviour, and a spontaneous process under ambient conditions, related to the known carbonation mechanisms of these materials [16] in service.

Knowing these efflorescence mechanisms and the factors that influence them, it therefore remains to be established how efflorescence will affect the microstructure and properties of a geopolymer. To date, there has been very little direct investigation into this topic. From their leaching experiments, Škvára et al. [13] studied the MAS NMR spectra of alkali-activated fly ash and alkali-activated metakaolin, finding that Si and Al environments did not change when sodium concentration decreased, consistent with the observation that the majority of alkali cations in geopolymers are ion-exchangeable [17]. They attributed the strength reduction in geopolymer mortars immersed in water to the 'lower cohesion forces between the gel particles' instead of the loss of alkalis. Najafi Kani et al. [18] compared the compressive strengths of a set of geopolymer pastes, and found a close relationship between the leachable sodium and strength reduction. This suggests that the retention of sodium in geopolymers is beneficial for achieving or retaining high strength, but there are some aspects of the links between efflorescence, loss of alkalis from geopolymers, and mechanical performance, which remain unclear. Considering the differences in alkali loss rates and mechanisms between leaching and efflorescence processes, the influence of efflorescence on these important physical properties is particularly unclear.

Following our previous research on chemical processes related to efflorescence [15], this study focuses on the effects of efflorescence on material properties and performance. Direct comparisons between dry geopolymer products and those subjected to simulated efflorescence have been performed. This study aims to provide new understanding of the changes in phase assemblage, microstructure and mechanical properties of fly ash-based

geopolymer pastes through tests on samples with various fly ashes, activators and ageing/exposure conditions.

2. Experimental program

2.1 Materials

Three fly ashes obtained from Gladstone, Callide and Millmerran power stations (QLD, Australia) were used in this study, denoted as A, B and C. Compositional analysis using X-ray fluorescence (XRF; Table 1) shows that the three fly ashes contain high concentrations of SiO_2 and Al_2O_3 and low levels of CaO, typical of Australian hard coal fly ashes [19]. Considering this compositional information, as well as their particle sizes determined using a laser particle analyser (Malvern Mastersizer 2000) with wet dispersion (Fig.1), the three fly ash samples can all be classified as Class F under ASTM C618 [20]. Previous manufacturing trials using these three fly ashes, and also those by other authors who used fly ashes from the same sources, prove that they are suitable for geopolymer synthesis, but with different L/S ratios giving desirable performance for each ash [7]. This is mainly due to their differences in particle geometry. As it can be seen in scanning electron scanning micrographs (SEM; JEOL JCM-6000; high vacuum operation, 15 kV accelerating voltage, samples coated with gold, Fig. 2), fly ash C contains more large irregular particles and few very fine particles, and in mixing it needs a relatively higher L/S ratio than fly ashes A and B to achieve equivalent workability. In addition, fly ash A shows to have the smallest average particle size, and is expected to require the lowest liquid phases and generate the highest compressive strength due to better packing and nucleation. To minimise binder porosity, a minimal liquid content (including the additional water) was used for each sample. The resulting pastes exhibited comparable flowability (Table 2).

Activator type is an important factor affecting efflorescence rate [15]. To better understand the consequent influences of efflorescence on geopolymer properties, two activators were used: an NaOH solution and a sodium silicate solution. The NaOH solution (abbreviated as NH) was prepared by dissolving NaOH pellets (99% purity, Formosa Plastics Corporation, Taiwan) in water to a concentration of 12 mol/L. The sodium silicate solution (abbreviated as $NS_{1.5}$) was prepared by mixing NaOH, D-Grade^{TM} liquid sodium silicate (PQ Australia Pty. Ltd., with original modulus of 2.0) and water to a combined modulus of 1.5 and concentration of 35 wt.% activator solids (Na_2O+SiO_2). The activators were allowed to equilibrate to room temperature prior to use. Deionised water was used throughout all experiments. It is noted here that fly ash A and C are used study the effect of activator type while fly ash B was mixed at two activator/solid ratios to examine the effect of alkali concentration under the same type of activator.

2.2 Synthesis of geopolymers

Geopolymer paste mix proportions are given in Table 2. It should be noted that the Na_2O wt.% refers only to that which is supplied by the activator, excluding the small amounts originating from the fly ashes.

The pastes were poured into ø23 mm × 24 mm cylindrical moulds, vibrated to eliminate large air bubbles, and then sealed for initial 24 h of low temperature curing in an environmental chamber at RH = 90±10%, 25 ± 1°C. After that, the chamber temperature was increased to 75 ± 1°C within a period of 15 min, held for 12 h, and naturally cooled down to 25 ± 1°C, where it was held for a further 7 days. This particular curing regime was developed to achieve high maturity of the fly ash geopolymers, according to the experience gained in other studies [13, 21]. Applying higher temperatures or longer curing periods is expected to have limited influence on the overall efflorescence potential [15, 18].

To investigate the structural evolution and mechanical properties of geopolymers associated with efflorescence, the demoulded specimens were subjected to 28 days of ageing under the following conditions:

a) In ambient air at 20 $\pm$ 5°C with RH varying from 20 to 60%;

b) In ambient air with the bottom immersed in water at a depth of 0.5-1 mm (water was refilled by drops every 2 to 3 hours);

c) Fully immersed in water at 20 $\pm$ 5°C.

The three ageing conditions simulated the service under dry, efflorescence (due to the access to both water and drying actions) and leaching conditions, respectively.

In addition, two low-strength geopolymers were prepared: one was a foam geopolymer, FGPC, was prepared by mixing prepared foam with fresh GPC-NS$_{1.5}$ paste [15] and followed the curing procedure described above. The other geopolymer with the mix proportions as GPC-NS$_{1.5}$ but cured at low temperature (20 $\pm$ 5°C), marked as LGPC.

2.3 Testing and characterization

Compressive strengths of aged samples were tested using an MTS universal mechanical testing machine at a loading speed of 0.5 mm/min. Before testing, the fully immersed samples and those with the bottom immersed were removed from the water, cleaned with tissue paper and conditioned in ambient air for 6 h. Each mixture had 4 to 5 samples tested, to obtain a mean value. The stress-strain curves were recorded to enable calculation of the compressive modulus of selected geopolymer pastes. Normally, the calculation of modulus of elasticity of concrete uses the stress from 50 millionths up to 40% of the ultimate load [22]. In this study, the small paste specimens were tested with several sheets of paper acting as a cap on the top surface, to minimise errors due to uneven surfaces. Thus, the initial deformation can be partially attributed to the deformation of the paper cap. Therefore, the

compression modulus was calculated by linear regression of the stress-strain curve between 30 to 70% of ultimate load, which was the region where the best linear regression could be obtained. This may lead to a higher value compared to using the standard method [22], but is acceptable for comparative purposes.

The fractured samples were collected for evaluation of efflorescence potential, open porosity and microstructure. The evaluation of efflorescence potential followed the leaching method described in [15]. Open porosity was determined using a vacuum saturation method, which has been shown to be effective in measuring the permeable porosity of cement-based concrete [23]. The fractured as-cured samples were crushed into 5 mm thickness particles, which were cleaned using compressed air and dried in an oven at 105°C for 24 h, to reach constant weight. The samples were allowed to cool to room temperature in a desiccator and then removed quickly, one by one, to determine the dry mass M_1. Then they were put in a vacuum desiccator at -90 kPa for 4 h, then soaked in boiled water with vacuum still running until they were fully immersed. The saturated surface-dry mass M_2 and the buoyant mass M_3 were weighed and the open porosity was calculated using eq.3:

$P= (M_2-M_1)/(M_2-M_3)\times100\%$ (Eq.3)

The air aged specimens and those after the simulated efflorescence program were selected for SEM analysis. The surface part was collected, dried at 65°C for 6 h and solidified in a resin, polished on a grinding-and-polishing machine (2000Cw silicon carbide waterproof abrasive paper) using several drops of acetone. The loose particles on the flat section were removed in acetone using an ultrasonic washer. The samples were dried at 65°C for 3 h and coated with gold for SEM analysis.

XRD data were collected using a Thermo Scientific ARL 9900 Series X-ray workstation with Co K_α radiation, operated at 40 kV and 40 mA, with a step size of 0.02° and a count time of 4

s/step, from 8 to 80° 2θ. FTIR analysis was performed using a Shimadzu IR Prestige-21 workstation with the KBr pellet method. The samples aged in air and those showing intensive efflorescence in contact with water were selected for FTIR testing. The efflorescence products on the surface were gently removed and tested, then the skin part (less than 2 mm in thickness) was scraped from the samples, ground and dry mixed with KBr to prepare the testing pellets. The efflorescence and subflorescence products were also analyzed by FTIR.

3. Results and discussion

3.1 Efflorescence of geopolymer pastes

3.1.1 Visual observation

Visual observation is the most direct method by which efflorescence of geopolymers can be identified. Fig. 3 depicts the samples under the simulated efflorescence conditions, i.e. in contact with water at the bottom. GPA-NS$_{1.5}$ does not show any evidence of efflorescence on the surface up to 24 hours, while in contrast, GPA-NH starts showing visible efflorescence products in 2 hours. The products deposited on the surface of this sample became more evident at 3 hours, as shown in the photographs in Fig. 3, and continued to grow throughout the observation period. The much slower efflorescence of GPA-NS$_{1.5}$ is believed to be related to its lower porosity than GPA-NH, as the activator contains soluble silicate. This can be seen in Fig. 4. The open porosity of GPA-NS$_{1.5}$ is 23.4% while it is 26.8% in GPA-NH. High porosity of the hardened binder is one of the key properties that can lead to rapid efflorescence [15]. However, in comparison, GPB-NS$_{1.5}$(H), which is activated using the same activator as GPA-NS$_{1.5}$, shows much more rapid efflorescence, just because the fly ashes sourced differently. It is noted that the GPB-NS$_{1.5}$(H) has lower porosity than GPA-NS$_{1.5}$. This result indicates that the properties of the fly ash have a significant influence on the efflorescence behaviour. Fig.1 shows that compared to fly ashes B and C, fly ash A has

more particles smaller than 4 μm, which are expected to be highly reactive [24], and so the derived GPA-NS$_{1.5}$ may have a higher reaction extent, leaving less free alkalis in the matrix. This highlights that the severity of efflorescence could be different from case to case when geopolymers are made with different fly ashes, even when the activation conditions are the same.

The most rapid efflorescence occurs on the surface of GPB-NS$_{1.5}$(L): tiny white products are observable after 1.5 hours (not shown), and after only 3 hours, evident efflorescence products can be seen on its surface above the wet line. This is in agreement with the highest open porosity of GPB-NS$_{1.5}$(L) (Fig.4). This result indicates that lowering the alkali concentration in a geopolymer by reducing the amount of sodium silicate activator may not be a good practical method to mitigate efflorescence, if it leads to an inadequate microstructural development.

Both GPC-NS$_{1.5}$ and GPC-NH appear wet on the surface rapidly when they are placed in contact with water at the bottom, showing the high rate of capillary uptake. Thus, they do not show visible efflorescence products immediately, due to the dissolution of sodium carbonates before they can form on the wet sample surface. The top surface remains relatively dry, and exhibits efflorescence after 3 hours, particularly for GPC-NH (Fig.5). The crystal clusters on the top surface of GPC-NH have grown into a relatively large particle and become transparent. In addition to the previous observation that efflorescence can occur within the near-surface pores of a geopolymer matrix [15], this study shows that efflorescence may not be immediately evident to visual inspection due to dissolution into the surface liquid, or due to growth into large but transparent crystals. Leaching analysis will give more accurate information about the efflorescence potential of the samples.

Fig.6 shows the degree of Na leaching from the monosized geopolymer particles as a function of time as determined by atomic absorption spectroscopy. The efflorescence

potential, as indexed by the sodium leaching extent, varies significantly when different fly ashes and activators are used. It is not surprising to find that GPA-NS$_{1.5}$ leaches Na$^+$ more rapidly than GPA-NH in the testing period; in previous work, it was found that at the same alkali concentration, a sodium silicate activated geopolymer leached Na$^+$ more rapidly and to a greater extent than a comparable sodium hydroxide activated sample [15]. However, a higher efflorescence potential as measured in leaching tests does not necessarily lead to faster efflorescence. In this study each monolithic specimen is cracked into monosized fractured particles (1.25-1.50 mm), dried at and the surface exposed to water increases by a factor of ~100 compared to the monolith tests, so the leaching of Na$^+$ is greatly accelerated, with porosity effects showing reduced significance. This procedure was applied in a previous study and was confirmed to be effective

GPA-NH releases much less Na$^+$ in the leaching tests, and at a slower rate, than GPC-NH, although these two geopolymer pastes contain the same concentration of Na$_2$O (Table 2). This leaching result, which is in agreement with the visual observation results, indicates that the nature of the fly ash has a significant impact on the efflorescence behavior of geopolymers. This is also demonstrated by the much higher leaching of Na from GPB-NSi$_{1.5}$(H) after 72 hours than from GPA-NaS$_{1.5}$, which has the same alkali concentration. GPC-NS$_{1.5}$, which contains less alkalis than GPA-NS$_{1.5}$ and GPB-NS$_{1.5}$(H), leaches even higher concentrations of Na$^+$.

3.2 Effects of efflorescence on phase and pore structure

3.2.1 Microstructural analysis

The effect of efflorescence on geopolymer phase evolution can be observed by XRD (Fig. 7). For the geopolymers derived from fly ash A, the patterns do not show notable differences

between GPA-NS$_{1.5}$ samples (Fig.7a) after the three ageing programs. The crystalline phases

mullite (Al$_{4.52}$Si$_{1.48}$O$_{9.74}$), quartz, hematite and magnetite detected in the raw fly ash are still

present. The GPA-NH samples (Fig.7b) contain some hydroxysodalite (Na$_4$Al$_3$Si$_3$O$_{12}$(OH)), a

common zeolite-like phase formed in alkali-fly ash systems [25, 26]. Retention of alkalinity

in geopolymers is beneficial to achieve further reaction of residual precursors for an extended

period after hardening, so a lower extent of reaction is expected under the leaching conditions

due to the loss of alkalis. However, the diffraction patterns of the samples under the three

conditions are almost the same. Sodium carbonate phases were expected to be seen in the

binders [18, 25], but do not appear in the patterns here. There are two possible reasons: either

the majority of the efflorescence product has been removed from the surface before sampling,

and/or the concentration of sodium carbonate in the surface layer tested is below the detection

limit of the XRD method, as the total Na$_2$O concentration is only 3.5-6.2%.

From Fig. 7c and d, the increase in Na$_2$O concentration from 3.9% in GPB-NS$_{1.5}$(L) to 4.6%

in GPB-NS$_{1.5}$(H) does not change the mineralogical characteristics of the resulting

geopolymer. In each ageing group, the efflorescence does not change the main components,

including the dominant amorphous phase along with residual mullite (Al$_{2.272}$Si$_{0.728}$O$_{4.864}$),

quartz and magnetite. There is no carbonate or new phase observed after the simulated

efflorescence program.

The GPC-NS$_{1.5}$ samples (Fig.7e) which show the most intensive efflorescence do not have

detectable phase change after the simulated efflorescence program. In GPC-NH (Fig.7f) the

two weak diffraction peaks at 10.68° and 33.84° 2θ show the formation of chabazite-Na

(NaAlSi$_2$O$_6$·3H$_2$O) after ageing in contact with water. This zeolite was also identified in 8 M

NaOH-activated fly ash mortars after curing at 85°C for 20 h [25]. This again testifies that

high humidity is helpful for the crystallisation of alkali aluminosilicate gels during curing and

ageing [27]. Except for this humidity-induced formation of chabazite-Na, however, the

sample after the simulated efflorescence test does not show notable phase changes in comparison with the ambient air aged sample. From the diffraction analysis it is reasonable to conclude that the efflorescence-inducing conditions have very limited effect on the mineralogical characteristics of the geopolymer itself.

Fig.8 shows the microstructures of the near-surface part of the geopolymer samples after ageing in ambient air and the efflorescence layer (8-10 mm higher than wet front) with the bottom of the sample immersed. The cross-section of GPA-NS$_{1.5}$ after the simulated efflorescence program shows a more compact microstructure than is observed after ageing in ambient air. This is due to the availability of water when the bottom is immersed; the moisture in the matrix extends the period of reaction of the raw materials, refining the pore structure. Conversely, the cross-sections of GPA-NH and GPC-NH after the simulated efflorescence programme are coarser when compared to their corresponding samples after ageing in ambient air. Given that the same polishing and washing procedures were used for all of the samples, the coarse microstructure in cross-section implies the binder may be soft or less strong. The loss of alkalis due to the intensive efflorescence in these two binders is likely to be harmful to the strength development, and this will be explored in more detail in section 3.3.

GPB-NS$_{1.5}$(H) and GPC-NS$_{1.5}$ show the formation of large pores after the simulated efflorescence programme. It has been reported that under the high temperature ageing conditions, the transformation of amorphous geopolymer gels synthesised from metakaolin into zeolites is accompanied by the formation of large pores in the binder; however, the pore structure of the binder derived from fly ash does not form distinct large pores [28]. The ageing in contact with water induces the formation of zeolite-like crystalline phases (Fig.7), but the extent of crystallisation is much lower than was observed in [28]. Therefore, the most likely reason for the increased volume of large pores is that the later reaction (during ageing)

was affected in the specimens displaying intense efflorescence. As the residual alkalis in the matrix are transported and consumed by the deposition of $Na_2CO_3 \cdot nH_2O$ on the sample surface, the ongoing reaction is reduced, resulting in less strong (or less volume of) gels compared to the ambient air aged specimens. Additionally, some of the residual ash particles may not be strongly bonded and could fall out during polishing. If this is true, the mechanical strength of the GPB and GPC mixes, which show intensive efflorescence in contact with water, may be affected.

The efflorescence products of GPC-NS$_{1.5}$ were also examined by SEM (Fig. 9). The products formed on the surface of GPC-NS$_{1.5}$ after 28 days of ageing in air (Fig. 9a) grow from flat crystals tightly adhering to the binder into needle-like clusters. Similar crystals were found on the surface of fracture of air-aged GPC-NS$_{1.5}$ (Fig. 9b), which are identified as the products of carbonation during sampling. Without rigorous EDS re-examination on these crystals, it is difficult to confirm their compositions; however, as captured and determined in many previous studies [13, 15], these crystals show typical morphology of hydrous sodium carbonates.

3.2.2 FTIR analysis

FTIR method was used to analysis the effect of efflorescence on the T-O (T=Al or Si) bonds in the GPB and GPC which have been subjected to intensive efflorescence in contact with water (Fig.10). The broad band shifts from 1085-1092 cm^{-1} in the original fly ashes [7] towards lower frequencies is regarded as a signal of the formation of geopolymeric gels. The broad band is ascribed to Al(Si)-O-Si asymmetric stretching vibrations for the geopolymeric gels. In a comparison of the vibration band shown in Fig.10, two differences are noticed: (1) the main bands locate at higher frequencies in the water contacted samples (this trend is not clear in GPC-Na$_2$SiO$_3$); (2) the main vibration bands intensify in the spectra for air aged

samples. These differences provide some evidences that efflorescence has affected the geopolymeric gels.

Škvára et al. [13] proposed that the lost Na^+ cations can be replaced by H_3O^+ under leaching conditions, without influence on the Al-O-Si backbone. However, under the efflorescence conditions, the FTIR analysis in this study indicates that the loss of OH^- and Na^+ due the growth of sodium carbonate may affect Al(Si)-O-Si bands. As indicated by Eq. 1 &2, efflorescence can be regarded as a neutralization process with the consumption of residual OH^- and Na^+ in geopolymeric gels, including pores. For an incomplete reaction system, holding a certain amount of alkalis in geopolymer binder is expected to drive the later reaction (during the 28 days of ageing), which could be extremely slow though as indicated by the very similar XRD patterns between air and water-contacted aged sample. If the alkalis are diffused and depleted due to efflorescence, the formed gels will contain higher Si concentration, on an average level, due to the less incorporation of Al dissolved from fly ash. As a result, the stretching of Al(Si)-O-Si bonds in efflorescence samples will vibrate at higher wavenumbers, compared with those in air aged samples, and also at a relatively lower intensity due to less gel formed. These theoretical expectations agree with the findings in Fig. 10. In the carbonation of high calcium systems (Portland cement, alkali-activated slag), the main vibration band of Si-O was noted to shift slightly towards higher wavenumbers, which was attributed to the decalcification of the C-S-H gel [29-30]. Considering the nature of efflorescence, a process involving carbonation, dealumination and/or loss of sodium could exist and cause the shift of band positions in Fig. 10. However, the very slight shift, compared to the large shift observed in the high calcium systems [29-30], indicates that the chemical composition of the gels is only lightly affected by efflorescence. According to above SEM, XRD and FTIR results, efflorescence in geopolymer does not change the main

mineralogical compositions but likely restricts the later reaction of fly ash after hardening and this is expected to be harmful to the strength development.

3.3 Effects of efflorescence on mechanical properties of geopolymers

3.3.1 Compressive strength and modulus

The effects of efflorescence on the mechanical properties of geopolymer pastes are important with regard to the durability of geopolymer concretes. Fig. 11 shows the compressive strength development of geopolymers under the three ageing conditions after demoulding. The hardened pastes have achieved varying strengths at the time of demoulding, depending on the source of fly ash, the type and dosage of activator, and the additional water used to equalise flowability. The geopolymers derived from fly ash A exhibit higher strengths than the other two groups, at either the same dosage of sodium silicate (GPA-NS$_{1.5}$ compared to GPB-NS$_{1.5}$(H)) or the same dosage of NaOH (GPA-NH compared to GPC-NH). The more compact microstructures of GPA specimens as shown in Fig.8 are likely to partially contribute to their high strengths. Although the reaction extent has not been examined, it is believed that GPA samples also have higher amounts of activation products because of smaller particles and higher concentration of network modifiers in glassy phases of fly ash [7]. As indicated by the data for GPC, sodium silicate activation can generate higher strength than NaOH activation, even when the latter is formulated to supply more Na$_2$O. The gels derived from high Si systems (usually by activation using alkali silicate solutions containing a high concentration of dissolved silicate) have better microstructure, that is less pores and more homogeneous appearance, in metakaolin systems [31-32] and fly ash systems [25, 33]. As expected, the decrease of activator dosage in GPB (from sample H to sample L) leads to a reduction in strength.

After 28 days of ageing, the compressive strengths of the pastes in air all increased by 20 to 35% of their demoulding strengths, while the fully immersed samples showed much less increase in strength compared to their strength at demoulding. Considering the conditioning process of all samples under the same RH conditions before compression testing, any possible errors due to the effect of differing moisture conditions could be small (it has been stated that '*In general, specimens have 5–20 % lower compressive strengths when tested in a moist condition than they would if tested in a dry condition*' [34]). So, this result provides evidence that is somewhat in conflict with the mechanism of 'lower cohesion forces between the gel particles' proposed by Škvára et al. [13]. The lower rate of strength increase for immersed samples is more likely due to the lower reaction extent due to the loss of alkalis into the water. It is evident that the loss of alkalis has a negative influence on the strength development of geopolymers. The samples under the simulated efflorescence conditions gain strength only to a very limited extent, if at all. The compressive strengths of GPA-NH and GPC-NH may be lower after 28 days than their respective demoulding strengths, but the results are within experimental uncertainty. However, these results do start to show the negative influence of efflorescence-inducing conditions on compressive strength development.

The values of the compressive modulus of elasticity of geopolymers as calculated from the measured strain-stress curves are also shown in Fig.11. The GPA-NS$_{1.5}$ samples by the three ageing conditions do not vary significantly in modulus. The modulus of GPA-NH in contact with water at the bottom is 25% lower than when aged in ambient air and 14% lower than the fully immersed conditions. This trend shows a close relationship between the compressive strength and modulus of the hardened geopolymer pastes, particularly for GPC. The low modulus of immersed samples shows the softening effect of contact with water, particularly when the samples are of low strength or modulus. In addition to this, the reason for the much

lower modulus of the samples in contact with water at one end compared to the other two ageing conditions is probably partially due to the effect of intensive efflorescence.

The negative influence of efflorescence is expected to be a combined effect of multiple factors, most critically (1) loss of alkalis and (2) subflorescence. Other factors associated with efflorescence, such as shrinkage, could also be partially responsible for the strength loss, but the determination of shrinkage is beyond the scope of this study; we focus here on the effects of loss of alkalis and subflorescence.

Firstly, it has been well acknowledged that the reaction extent of fly ash is usually below 50% in 'well matured' geopolymers [35, 36], possibly reaching 60% for some high Al fly ashes [37]. The residual fly ash can be ongoingly activated by free alkalis in pore solutions during the long period of ageing. However, when a geopolymer paste is placed in the simulated efflorescence conditions, water can be drawn into the pores of the solid matrix by capillary suction, and evaporate from the sample surface. The internal alkalis are thus carried towards the surface, providing Na^+ for the precipitation of sodium carbonates, until an equilibrium (saturation) condition between the pore solution and the crystals is reached. As mentioned above, the reduced alkali concentration in the matrix due to this migration will affect or suppress the later activation of residual precursors.

The second key factor, subflorescence, is defined as the precipitation of salts at depth, usually within pores, at drying front in a solid matrix, such as masonry and stone [2]. For a PC based material, subflorescence can be trigged by the supersaturation of pore solutions due to the diffusion of salts from outside environment or the species dissolved from cement and aggregates [38]. For the geopolymer in contact with water, subflorescence is induced by the reaction between the free alkalis and the CO_3^{2-} absorbed from the atmosphere. Unlike on the surface, where carbonate crystals are free to grow (Fig.9), subflorescence will generate a crystallisation pressure, which is the pressure exerted by the crystal on the surrounding solid

matrix. Whether this pressure in the pores will damage the matrix depends on its magnitude and the mechanical properties, specifically the tensile strength, of the matrix [38, 39]. In practice, when efflorescence occurs on building materials exposed to humidity and/or salty environments, subflorescence is often actually the reason for their degradation by expansion and cracking. This mechanism is interpreted in more detail in the following section.

3.3.2 Understanding of subflorescence

To illustrate the mechanical effects of subflorescence, the two low-strength geopolymer samples, FGPC and LGPC, were used to subject to simulated efflorescence. The FGPC achieved a compressive strength of 8 MPa with a density of 980 kg/m^3 at the time of demoulding. The LGPC achieved 15 MPa after being cured at room temperature for 28 days. Fig.12a shows a layer of whitish efflorescence products precipitated on the drying line of FGPC. Cracking and spalling of material is evident above this level. This is due to the subflorescence occurring at the drying front beneath the sample surface, as sketched in Fig.12c. The crystallisation stress exceeds the tensile strength of the porous material, resulting in the observed cracks. A similar mechanism is evident in the solid geopolymer sample LGPC shown in Fig.12b. However, subflorescence may be nondestructive if the material is strong enough to sustain the crystallisation pressure; in a long term inspection, the higher-strength (40 MPa) sample GPA-NS$_{1.5}$ showed efflorescence at the drying line but did not show any macroscopic cracks or spalling after being held in contact with water at the bottom for 180 days.

To better understand the relationship between the efflorescence and subflorescence occurring in geopolymers, the whitish crystals formed on the surface of LGPC and those grown under the spalled layer were collected and analysed using FTIR spectroscopy. Fig.13 shows that the products formed at the two depths are almost the same. The two strong absorption bands centred at 1453 and 865 cm^{-1} are attributed to asymmetric vibrations v_3 and v_2 of CO$_3^{2-}$

respectively [40]. The broad band 2976 to 3405 cm^{-1} is attributed to O-H stretching vibration in absorbed water [41]. The broad feature with overlapping sharp sub-bands at 1143 and 1068 cm^{-1} is due to the asymmetric stretch of Si-O-(Si/Al) bonds and the symmetric vibration v_1 of CO_3^{2-}. The bands at 687, 560 and 455 cm^{-1} are assigned to Si-O-Si symmetric stretch, O-Si(Al)-O bending and O-Si-O bending vibrations in TO_4 tetrahedra [25]. These Si-O and Al-O bonds belong to geopolymeric material collected along with the efflorescence and subflorescence products, which are identified as hydrous sodium carbonates, in agreement with [15]. The subflorescence occurring under the surface is thus due to the reactions between alkalis and the more deeply diffused CO_3^{2-}. This subflorescence can be regarded as an extended efflorescence but may lead to harmful effects on the material due to the generation of crystallisation pressure.

It is difficult to directly probe the crystallisation pressure in porous materials, such as the geopolymers here. It is also not straightforward to calculate precise theoretical values using the existing models (e.g. [38]), as the solubility of sodium carbonate is affected by a number of factors, such as pore size (or more precisely, pressure in pores) and temperature [42], and the actual concentrations of ions in the pores during drying is varying. Nonetheless, estimation of crystallisation pressure due to subflorescence is possible. The first required step is to define the likely crystallisation product among the various possible hydrates of socium carbonate. According to the phase diagram of $Na_2CO_3 \cdot nH_2O$ [43], it is reasonable to assume that in the drying pores the initially formed product is natron, $Na_2CO_3 \cdot 10H_2O$. In previous studies [15, 44], heptahydrate $Na_2CO_3 \cdot 7H_2O$ was detected in the efflorescence or carbonation product in the sodium silicate activated fly ash systems. The heptahydrate is preferred at lower relative humidities and could be directly formed if water evaporates from the pore solution very quickly; however, as subflorescence takes places under the surface while the samples are in contact with water, the humidity in the pores is expected to be very high. The

$Na_2CO_3 \cdot 7H_2O$ detected as an efflorescence product in [15] could be either formed directly due to the relatively low humidity on the surface where efflorescence takes place, or via transformation from natron [44]. Other possible phases, such as $NaHCO_3 \cdot nH_2O$ [11, 12], trace $Na_6(SO_4)(CO_3,SO_4) \cdot nH_2O$ [12] and $Na_3PO_4 \cdot 12H_2O$ [45], are not detected, so will not be considered here. Using the estimated liquid interfacial free energy (γ_{CL}=0.09 N/m) of $Na_2CO_3 \cdot 10H_2O$ [42] and eq. 4 describing the pressure in a confined spherical crystal with radius of r [38], the crystallisation pressure in a cylindrical pore can be approximated.

$$p = 2\gamma_{CL}/r \qquad\qquad\qquad (Eq.4)$$

The pore sizes in typical geopolymers are at a range of several nanometres to 2000 nm [46-48], as determined by mercury intrusion. The crystallisation pressure is therefore in the range 0.1-100 MPa. If the tensile strength of geopolymer products is 1 – 3 MPa [49], damage may be caused by crystallisation pressure due to subflorescence in pores below 120 – 360 nm. It is understood that the crystals may favourably grow in large pores (less confined), inducing low crystallisation pressure; however, under non-equilibrium conditions, the water evaporation in smaller pores can lead to high crystallisation pressures [38]. Felicetti and Lo Monte [50] reported that concrete explosive spalling is due to the interaction of (a) moisture and vaporization induced pore pressure and (2) thermal gradients and external load induced stress, and their specially designed hot-tension test confirmed that the pressure exerted inside of pores approximately equals to an intensification of the tensile stress. This is consistent with the theory of this study; unfortunately, the geopolymer samples after subflorescence have not been tested for tensile stress, thus a direct correlation between tensile stress and subflorescence induced stress (crystallization stress at different sizes of pores) is not obtained. However, it is believed that the impact of subflorescecne is not negligible in understanding the geopolymer fracture mechanism.

From the above analysis, unlike the case for efflorescence, the subflorescence can cause mechanical impact on the geopolymer matrix. The exact impact on the integrity of the samples, and particularly whether the process will be harmful or harmless, depends on the magnitude of the crystallisation pressure compared to the tensile strength of geopolymer matrix.

3.3.3 The relationship between efflorescence, subflorescence and carbonation

Considering the nature of the reactions, efflorescence and subflorescence in geopolymers are both fundamentally carbonation-related processes. However, there are differences between efflorescence, subflorescence and the normal carbonation processes. In calcium rich systems, the carbonation reaction takes place between dissolved CO_2 and free alkalis and alkali earth cations, and involves chemical damage to the binder structure itself through decalcification. In a fly ash geopolymer without significant levels of calcium, the chemical damage to the aluminosilicate matrix is much less obvious, and is not observable by NMR spectroscopy [44], and so it is quite possible that the loss of mechanical performance during carbonation is instead related to physical processes such as those described here. The consumption of free alkalis by carbonation in these materials is similar as efflorescence/subflorescence, which may occur at a relatively low humidity. The situation is likely to be very different from the case for higher-calcium binders, where the consumption of alkali earth cations through carbonation will change the Ca/Si ratios in the gel, and influence their mechanical properties [44]. The influence of crystallisation pressure on the two types of materials will also be different, as the voluminous sodium carbonate hydrate products formed in low-calcium geopolymer binders require more space than the anhydrous calcium carbonate polymorphs which form in calcium-rich systems.

There is also the possibility that other anions can contribute to the efflorescence and subflorescence processes if present in sufficient quantities; the ashes tested here have low

levels of phosphate and sulfate, but salts such as $Na_6(SO_4)(CO_3,SO_4) \cdot nH_2O$ [12] and $Na_3PO_4 \cdot 12H_2O$ [45] have also been identified in some fly ash geopolymers. So, it can be seen that the efflorescence, including subflorescence, occurring in alkali-activated systems is more than a simple carbonation process. It involves a process of consumption of free alkalis (or excessive alkalis) and perhaps other trace elements (such as sulphate and phosphate from fly ash or additives).

4. Conclusions

A broad efflorescence concept, including both deposition of carbonate products on the surface and subflorescence taking place under the surface, is proposed from examination of the microstructural and mechanical evolution of geopolymer pastes under laboratory ageing conditions. By using three fly ashes and two types of typical activators, it is found that the source of fly ash affects the efflorescence rate and potential significantly: the fly ash which requires relatively high L/S ratio to achieve high workability usually generates geopolymers with high porosity and consequently rapid efflorescence. Type of activator is less important than the fly ash source, in terms of affecting efflorescence rate of geopolymers. Due to the porosity changes, sodium silicate activated geopolymer can exhibit rapider efflorescence than those by sodium hydroxide; however, the efflorescence potential, as indexed by sodium leaching, is higher in the former.

Mineralogically, the efflorescence does not change the main components in the fly ash-based geopolymers, which consist of predominantly amorphous gels and residual crystalline phases that originated from fly ash. Small amount of zeolite phases are detected in the NaOH activated systems but are not affected by efflorescence. Efflorescence – or more specifically, loss of alkalinity and subflorescence – shows a negative influence on the compressive strength development, and also the compression modulus. From a long term of view, the loss of alkalis due to sodium carbonate precipitation on surface can affect the long-term ongoing

activation of residual aluminosilicate precursors in the hardened geopolymer. The subflorescence occurring under the surface of the geopolymers is due to the reactions between alkalis and the deeply diffused CO_3^{2-}, and can be regarded as an extended efflorescence. This subflorescence can generate a crystallisation pressure, which may lead to damage to the geopolymer matrix, depending on its magnitude and the tensile strength of geopolymer.

The results of this study suggest that the efflorescence occurring in fly ash-based geopolymers It is not only a 'skin problem' but also may lead to structural issues, particularly for systems with lower-strength and/or many free alkalis. Appropriate strategies must be considered in formulating and manufacturing geopolymers to eliminate this problem.

Acknowledgements

References

[1] A.M. Neville. Properties of concrete (5th edition). Pearson, London, UK. 2011.

[2] C. Dow, F.P. Glasser. Calcium carbonate efflorescence on Portland cement and building materials. Cem. Concr. Res. 33 (2003) 147–154.

[3] Z. Zhang, X. Yao, H. Zhu. Potential application of geopolymers as protection coatings for marine concrete I. Basic properties. Appl. Clay Sci. 49 (2010) 1–6.

[4] Z. Zhang, X. Yao, H. Zhu, Y. Chen. Role of water in the synthesis of calcined kaolin based-geopolymer. Appl. Clay Sci. 43 (2009) 218–223.

[5] P. Rovnaník. Effect of curing temperature on the development of hard structure of metakaolin-based geopolymer. Constr. Build. Mater. 24 (2010) 1176–1183.

[6] F. Pacheco-Torgal, D. Moura, Y. Ding, S. Jalali. Composition, strength and workability of alkali–activated metakaolin based mortars. Constr. Build. Mater. 25 (2011) 3732–3745.

[7] Z. Zhang, H. Wang, J.L. Provis. Quantitative study of the reactivity of fly ash in geopolymerization by FTIR. J. Sustain. Cement-Based Mater. 1 (2012) 154–166.

[8] E.I. Diaz–Loya, E.N. Allouche, S. Vaidya. Mechanical properties of fly–ash–based geopolymer concrete. ACI Mater. J. 108 (2011) 300–306.

[9] P. Chindaprasirt, T. Chareerat, S. Hatanaka, T. Cao. High-strength geopolymer using fine high-calcium fly ash. J. Mater. Civ. Eng. 23 (2011) 264–270.

[10] H. Szklorzová, V. Bílek. Influence of alkali ions in the activator on the performance of alkali-activated mortars. In: V. Bílek, Z. Keršner editors. The 3rd International Symposium on Non-Traditional Cement and Concrete. Brno, Czech Republic; 2008. pp. 777–784.

[11] F. Škvára, L. Kopecký, V. Šmilauer, L. Alberovská, L. Vinšová. Aluminosilicate polymers – influence of elevated temperatures, efflorescence. Ceram.–Silik. 53 (2009) 276–282.

[12] J. Temuujin, A. van Riessen. Effect of fly ash preliminary calcination on the properties of geopolymer. J. Hazard. Mater. 164 (2009) 634–639.

[13] F. Škvára, V. Šmilauer, P. Hlaváček, L. Kopecký, Z. CÍlová. A weak alkali bond in (N, K)-A-S-H gels: evidence from leaching and modeling. Ceram.–Silik. 56 (2012) 374–382.

[14] M.A. Smith, G.J. Osborne. Slag/fly ash cements. World Cem. Technol. 1 (1977) 223–233.

[15] Z. Zhang, J.L. Provis, A. Reid, H. Wang. Fly ash-based geopolymers: the relationship between composition, pore structure and efflorescence. Cem. Concr. Res. 64 (2014) 30–41.

[16] S.A. Bernal, J.L. Provis, D.G. Brice, A. Kilcullen, P. Duxson, J.S.J. van Deventer. Accelerated carbonation testing of alkali-activated binders significantly underestimates service life: The role of pore solution chemistry. Cem. Concr. Res. 42 (2012) 1317–1326.

[17] O. Bortnovsky, J. Dědeček, Z. Tvarůžková, Z. Sobalík, J. Šubrt. Metal ions as probes for characterization of geopolymer materials. J. Am. Ceram. Soc. 91 (2008) 3052–3057.

[18] E. Najafi Kani, A. Allahverdi, J.L. Provis. Efflorescence control in geopolymer binders based on natural pozzolan. Cem. Concr. Compos. 34 (2011) 25–33.

[19] C. Heidrich. Ash utilisation – an Australian perspective. 2003 International Ash Utilization Symposium. University of Kentucky, U.S.A., Paper #3.

[20] ASTM C618-08a. Standard specification for coal fly ash and raw or calcined natural pozzolan for use in concrete. 2008.

[21] D. Hardjito. Studies on fly ash-based geopolymer concrete. Curtin University of Technology, PhD thesis. 2005.

[22] ASTM C469/C469M – 14. Standard test method for static modulus of elasticity and Poisson's ratio of concrete in compression. 2014.

[23] Md. Safiuddin, N. Hearn, Comparison of ASTM saturation techniques for measuring the permeable porosity of concrete. Cem. Concr. Res. 35 (2005) 1008–1013.

[24] N.W. Chen-Tan, A. van Riessen, C.V. Ly, D.C. Southam. Determining the reactivity of a fly ash for production of geopolymer. J. Am. Ceram. Soc. 92 (2009) 881–887.

[25] A. Fernández-Jiménez, A. Palomo. Composition and microstructure of alkali activated fly ash binder: Effect of the activator. Cem. Concr. Res. 35 (2005) 1984–1992.

[26] N.M. Musyoka, L.F. Petrik, G. Balfour, W.M. Gitari, E. Hums. Synthesis of hydroxy sodalite from coal fly ash using waste industrial brine solution. J. Environ. Sci. Health. A: Tox. Hazard. Subst. Environ. Eng. 46 (2011) 1699–1707.

[27] J.L. Provis, G.C. Lukey, J.S.J. van Deventer. Do geopolymers actually contain nanocrystalline zeolites? A reexamination of existing results. Chem. Mater. 17 (2005) 3075–3085.

[28] R.R. Lloyd. Accelerated ageing of geopolymers. In J.L. Provis and J.S.J. van Deventer (Eds.) Geopolymers: Structure, Processing, Properties and Industrial Applications. Woodhead, Cambridge, UK; 2009. pp. 139–166.

[29] F. Puertas, M. Palacios, T. Vázquez. Carbonation process of alkali-activated slag mortars. J. Mater. Sci. 41 (2006) 3071–3082.

[30] S. A. Bernal, R.M. de Gutierrez, J.L. Provis, C. Rose. Effect of silicate modulus and metakaolin incorporation on the carbonation of alkali silicate-activated slags. Cem. Concr. Res. 40 (2010) 898–907.

[31] P. Duxson, J.L. Provis, G.C. Lukey, S.W. Mallicoat, W.M. Kriven, J.S.J. van Deventer. Understanding the relationship between geopolymer composition, microstructure and mechanical properties. Colloids Surf. A. 269 (2005) 47–58.

[32] Z. Zhang, H. Wang, J.L. Provis, F. Bullen, A. Reid. Quantitative kinetic and structural analysis of geopolymers. Part 2. Thermodynamics of sodium silicate activation of metakaolin. Thermochim. Acta. (565) (2013) 163–171.

[33] J.L. Provis, C.Z. Yong, P. Duxson, J.S.J. van Deventer. Correlating mechanical and thermal properties of sodium silicate-fly ash geopolymers. Colloids Surf. A. 336 (2009) 57–63.

[34] J.F. Lamond, J.H. Pielert. Significance of tests and properties of concrete & concrete-making materials. New York: ASTM International; 2006. pp. 132.

[35] P. Chindaprasirt, U. Rattanasak, C. Jaturapitakkul. Utilization of fly ash blends from pulverized coal and fluidized bed combustions in geopolymeric materials. Cem. Concr. Compos. 33 (2011) 55–60.

[36] A. van Riessen, N. Chen-Tan. Beneficiation of Collie fly ash for synthesis of geopolymer Part 2 - Geopolymers. Fuel 111 (2013) 829–835.

[37] A. Fernández-Jiménez, A.G. de la Torre, A. Palomo, G. López-Olmo, M.M. Alonso, M.A.G. Aranda. Quantitative determination of phases in the alkaline activation of fly ash. Part II: Degree of reaction. Fuel 85 (2006) 1960–1969.

[38] G.W. Scherer. Stress from crystallization of salt. Cem. Concr. Res. 34 (2004) 1613–1624

[39] N. Shahidzadeh-Bonn, J. Desarnaud, F. Bertrand, X. Chateau, D. Bonn. Damage in porous media due to salt crystallization. Phys. Rev. E 81 (2010) 066110.

[40] P. Lu, Q. Li, J. Zhai. Mineralogical characterizations and reaction path modeling of the pozzolanic reaction of fly ash-lime systems. J. Am. Ceram. Soc. 91 (2008) 955–964.

[41] S.S. Kouassi, M.T. Tognonvi, J. Soro, S. Rossignol. Consolidation mechanism of materials obtained from sodium silicate solution and silica-based aggregates. J. Non-Cryst. Solids 357 (2011) 3013–3021.

[42] L.A. Rijniers, H.P. Huinink, L. Pel, K. Kopinga. Experimental evidence of crystallization pressure inside porous media. Phys. Rev. Lett. 94 (2005) 075503.

[43] C. Shi, P.V. Krivenko, D Roy. Alkali-activated cements and concretes. Taylor & Francis, Abingdon, UK, 2006. pp. 7.

[44] S.A. Bernal, J.L. Provis, B. Walkley, R. San Nicolas, J.D. Gehman, D.G. Brice, A.R. Kilcullen, P.Duxson, J.S.J. van Deventer. Gel nanostructure in alkali-activated binders based on slag and fly ash, and effects of accelerated carbonation. Cem. Concr. Res. 53 (2013) 127–144.

[45] J. Temuujin, A. van Riessen, R. Williams. Influence of calcium compounds on the mechanical properties of fly ash geopolymer pastes. J. Hazard. Mater. 167 (2009) 82–88

[46] Sindhunata, J.S.J. van Deventer, G.C. Lukey, H. Xu. Effect of curing temperature and silicate concentration on fly-ash-based geopolymerization. Ind. Eng. Chem. Res. 45 (2006) 3559–3568.

[47] F. Škvára, L. Kopecký, J. Nìmeèek, Z. Bittar. Microstructure of geopolymer materials based on fly ash. Ceram.–Silik. 50 (4) (2006) 208–215.

[48] G.S. Ryu, Y.B. Lee, K.T. Koh, Y.S. Chung. The mechanical properties of fly ash-based geopolymer concrete with alkaline activators. Constr. Build. Mater. 47 (2013) 409–418.

[49] P. Yellaiah, S.K. Sharma, T.D. Gunneswara Rao. Tensile strength of fly ash based geopolymer mortar. ARPN J. Eng. Appl. Sci. 9 (11) (2014) 2297–2301.

[50] R. Felicetti, F. Lo Monte, Concrete spalling: Interaction between tensile behaviour and pore pressure during heating. MATEC Web of Conferences, 6 03001(2013) DOI:10.1051/matecconf/20130603001.

Fig.1. Particle size distributions of fly ashes A, B and C.
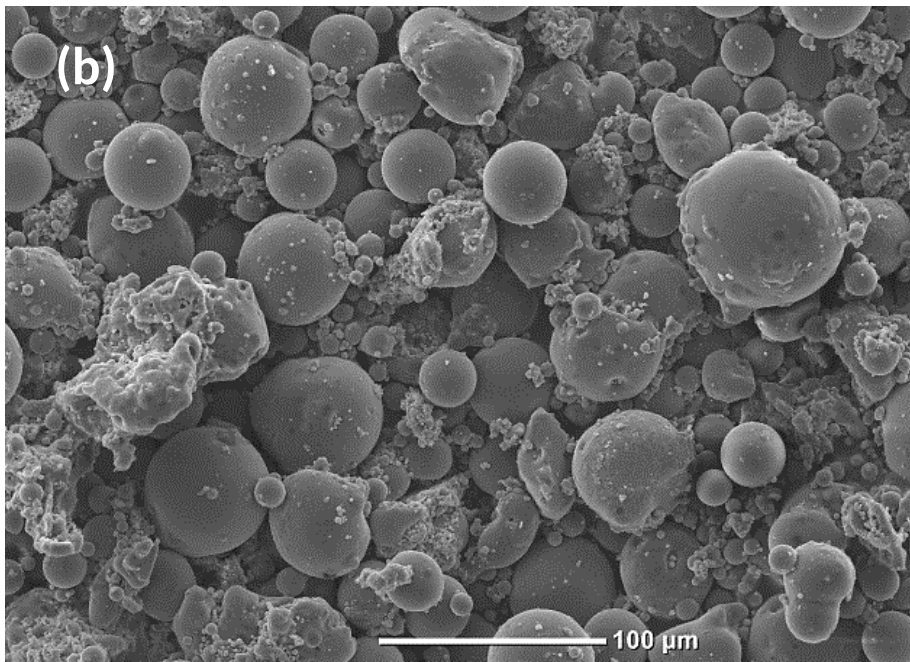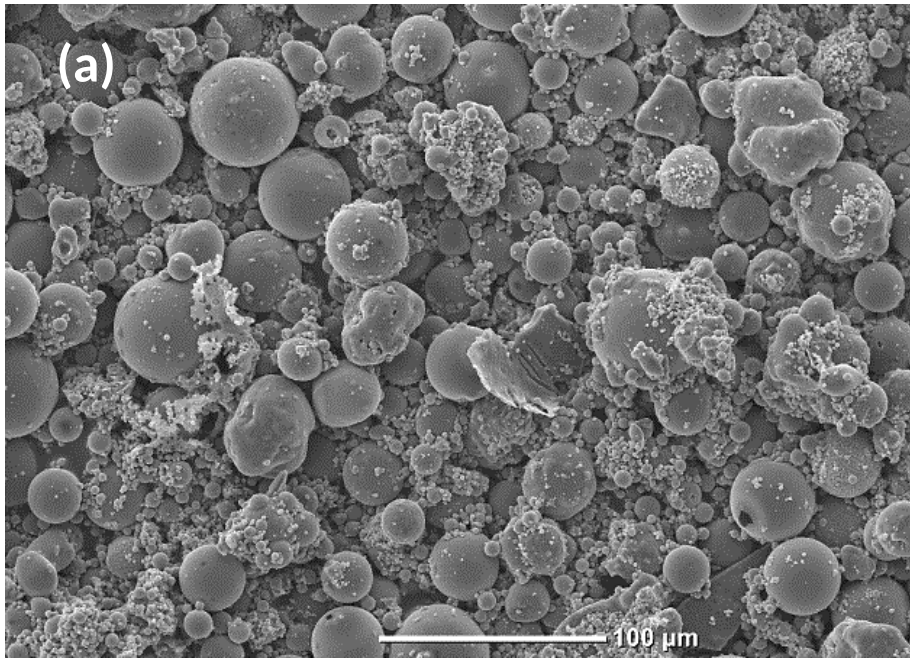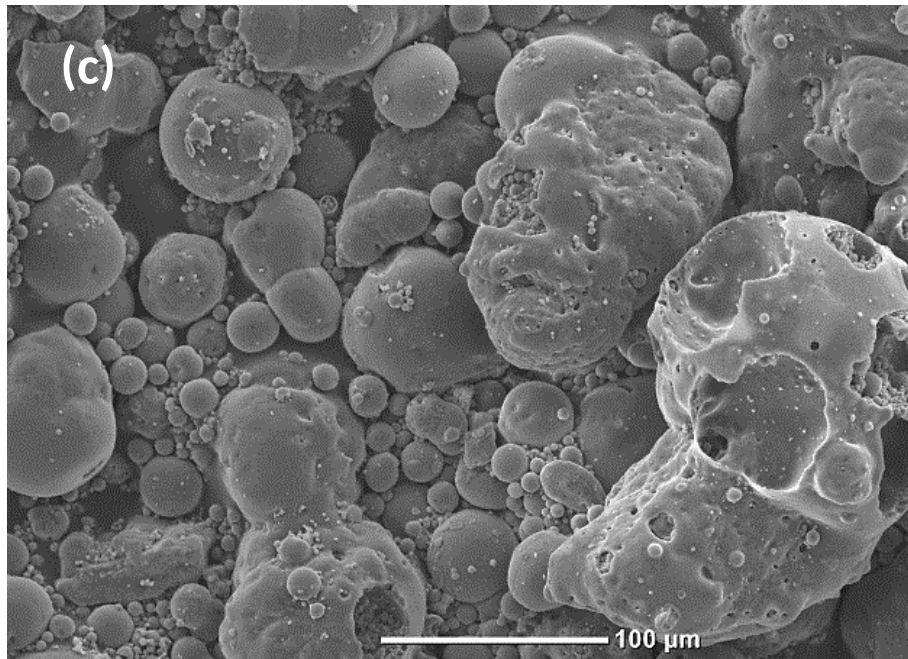
Fig.2. Particle morphologies as determined by secondary electron imaging in an SEM:
(a) fly ash A; (b) fly ash B and (c) fly ash C.

	GPC-NH	GPC-NS$_{1.5}$	GPB-NS$_{1.5}$(H)	GPB-NS$_{1.5}$(L)	GPA-NH	GPA-NS$_{1.5}$
0 hour						
3 hours						
24 hours						

Fig. 3. Efflorescence of hardened geopolymer pastes in contact with water at bottom at a depth around 1 mm.
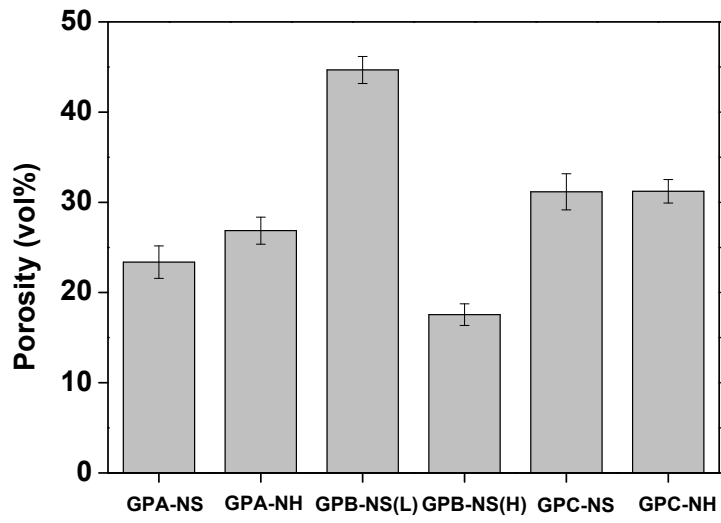
Fig.4. Porosities of geopolymer pastes as determined by vacuum saturation method.

Fig. 5. Large and transparent efflorescence products appear on the drying top surface of GPC-NH, after 3 hours in contact with water at bottom.

Fig. 6. The leaching of sodium from fractured geopolymer particles (1.25-1.50 mm) in deionised water at a solid/water ratio of 1:50 at 25°C. The samples have been dried at 65°C for 24 hours to reach a constant weight before testing.
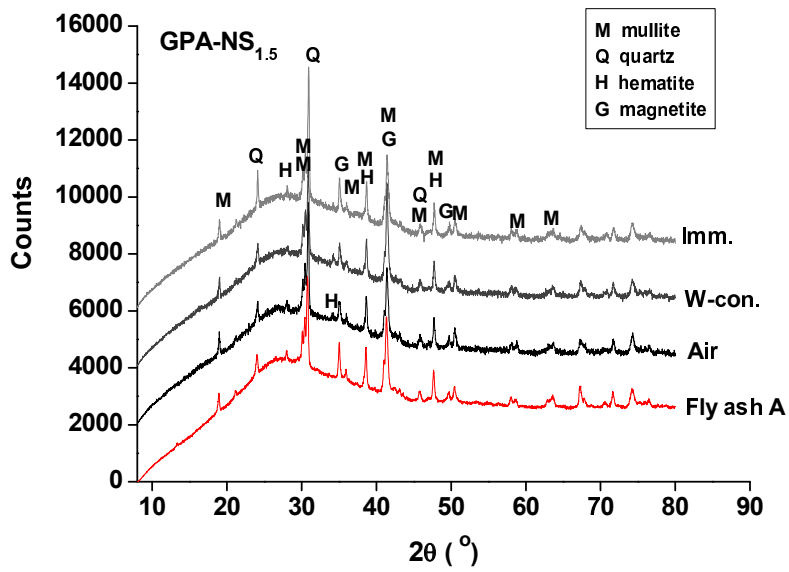
(a)
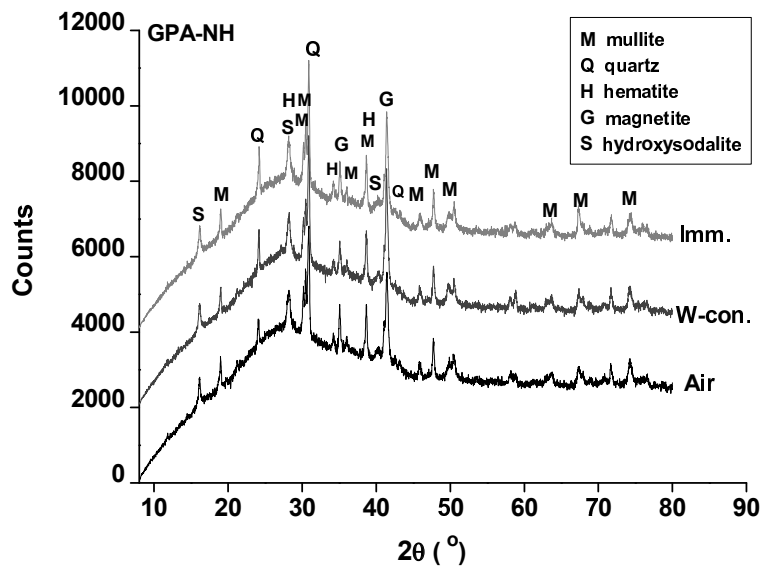
(b)
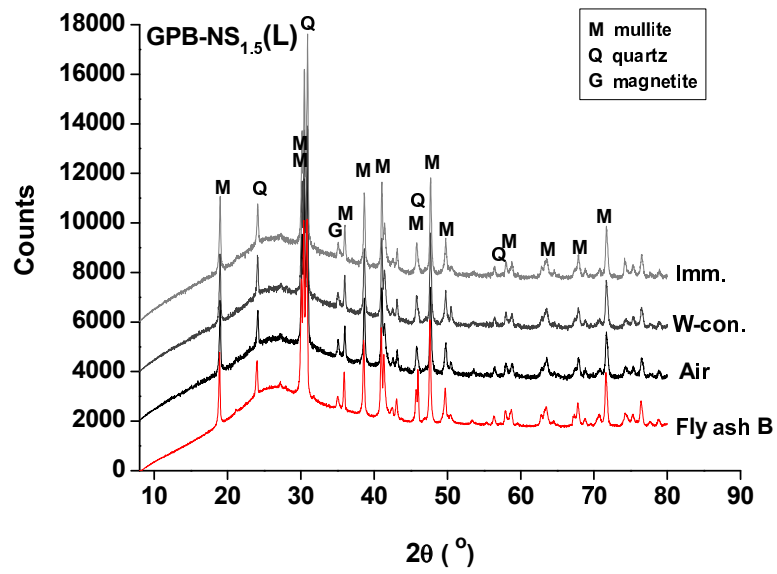
(c)
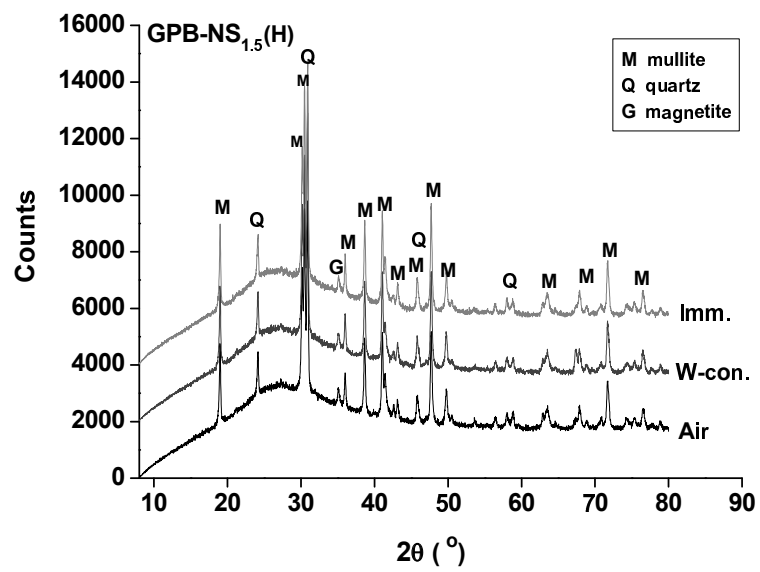
(d)
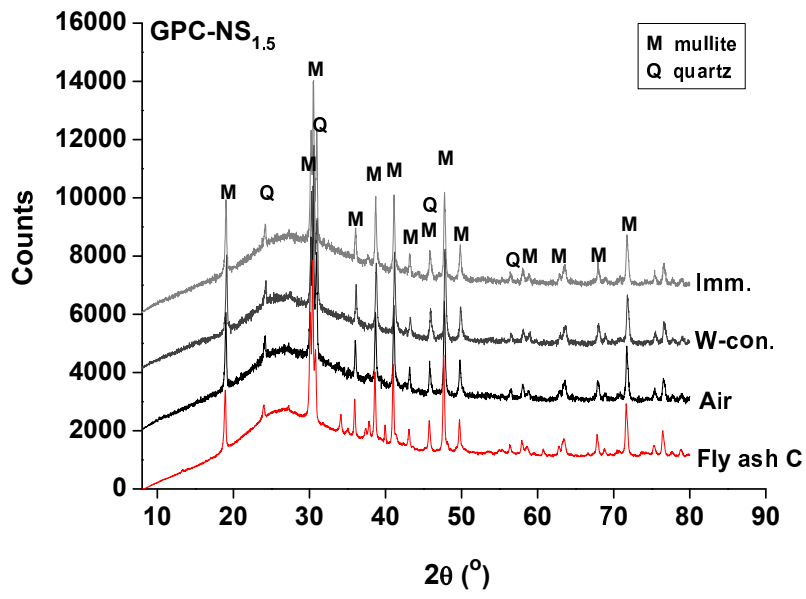
(e)
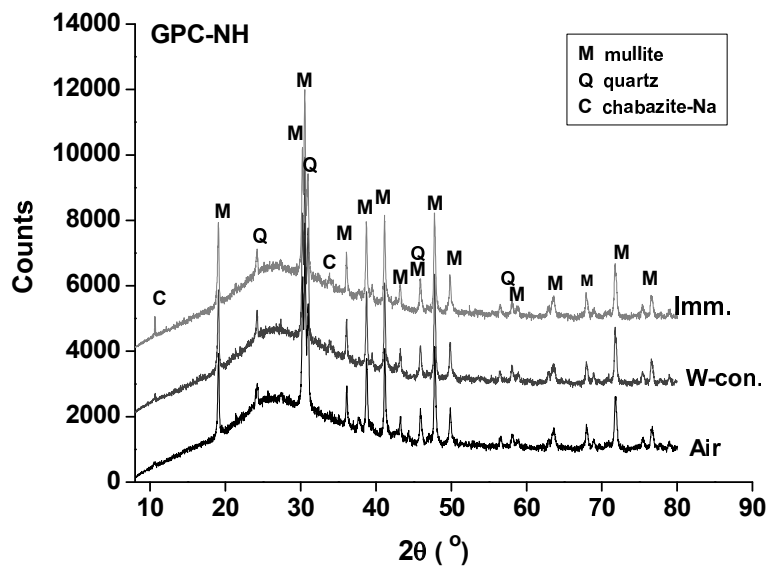
(f)

Fig. 7. XRD patterns of each fly ash, and of the hardened geopolymers after 28 days of ageing under conditions of ambient air (Air), in contact with water at bottom (W-Con.) and fully immersed (Imm.): (a-b) GPA, (c-d) GPB and (e-f) GPC.
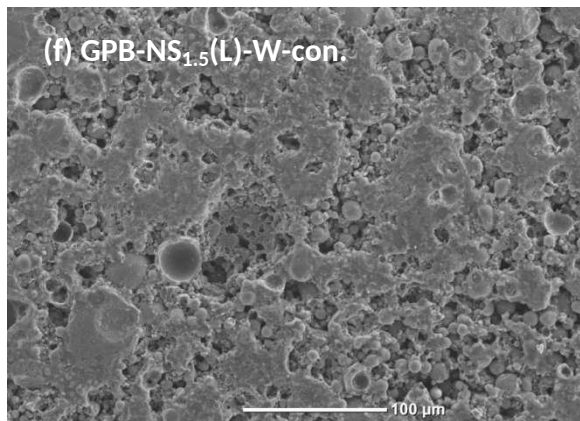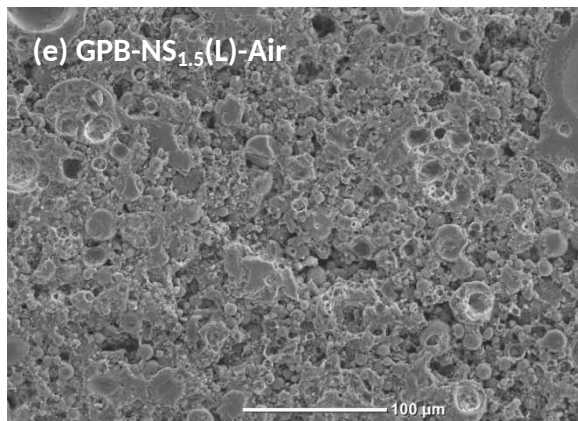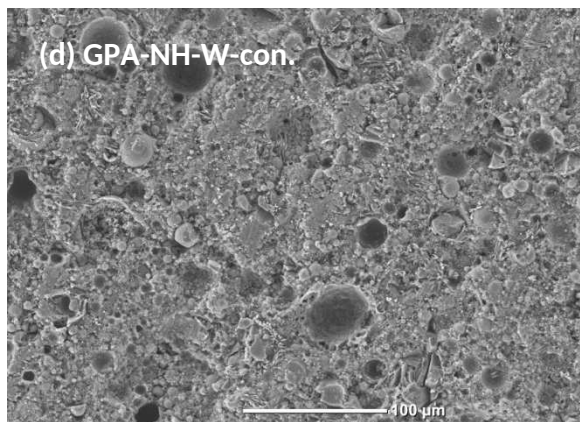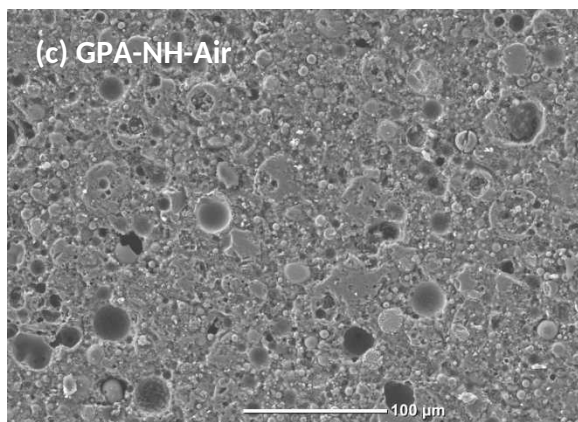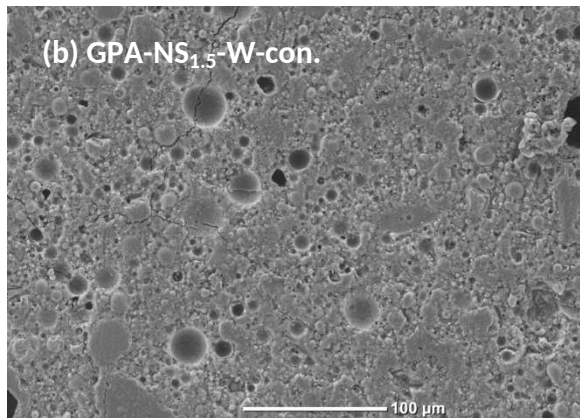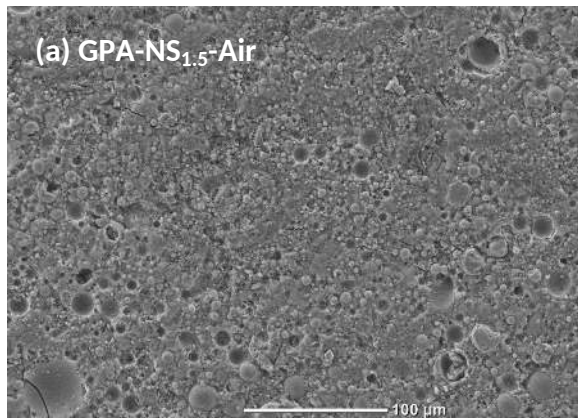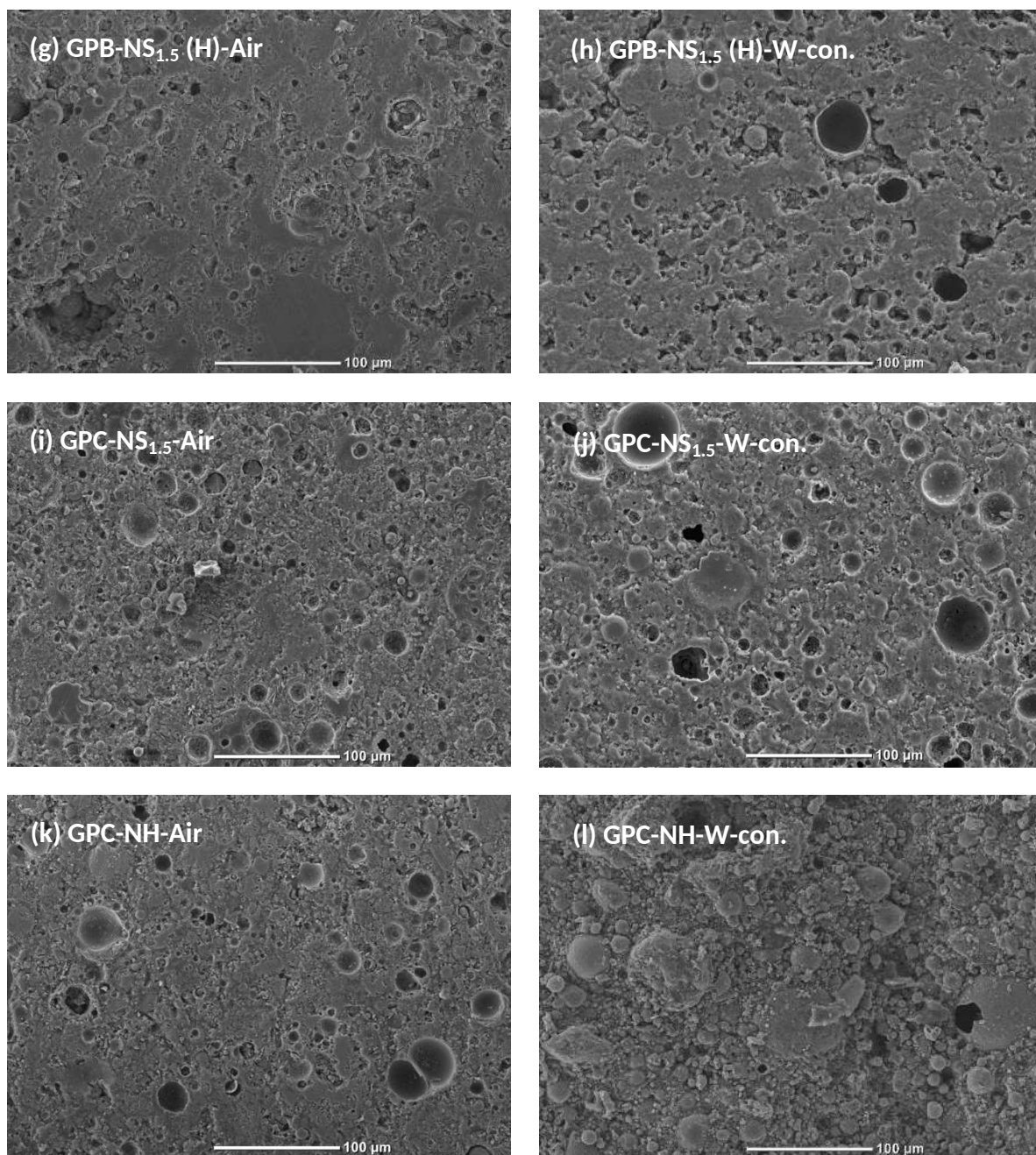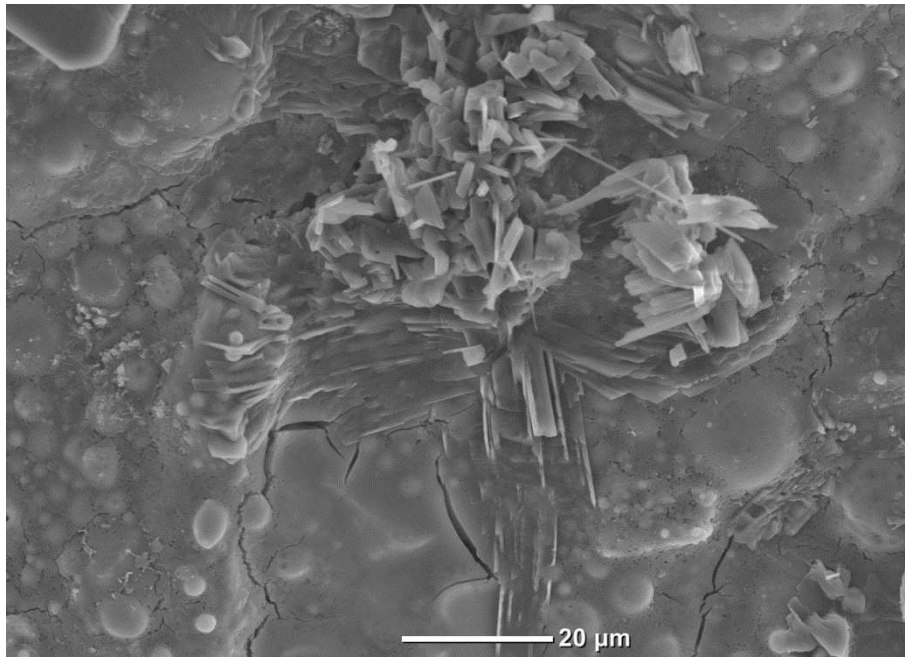
(a) GPA-NS$_{1.5}$-Air

(b) GPA-NS$_{1.5}$-W-con.

100 µm

100 µm

(c) GPA-NH-Air

(d) GPA-NH-W-con.

100 µm

100 µm

(e) GPB-NS$_{1.5}$(L)-Air

(f) GPB-NS$_{1.5}$(L)-W-con.
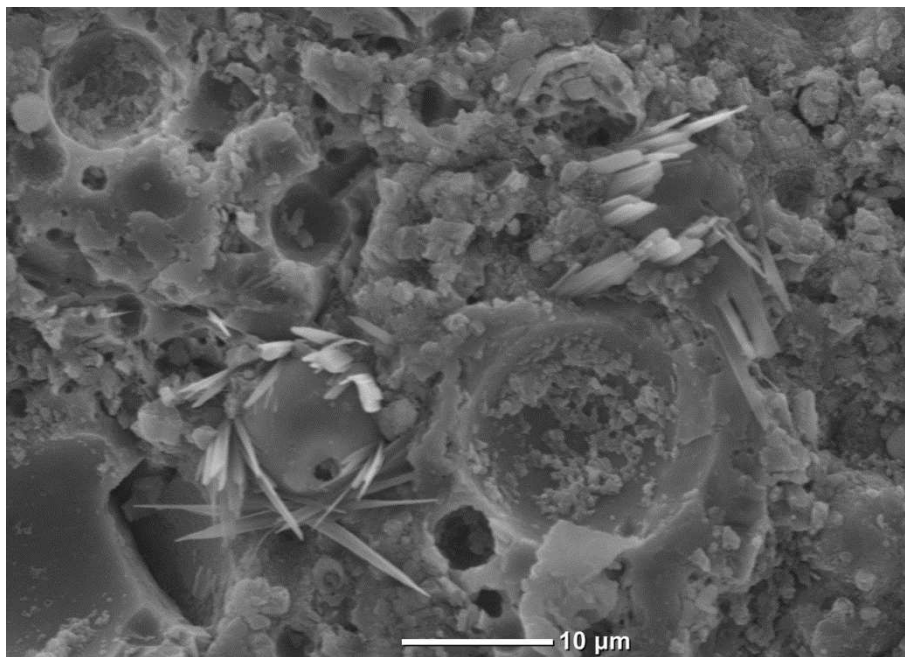
100 µm

100 µm

Fig. 8. SEM images of geopolymers after ageing in the ambient air (left) and in contact with water at the bottom (right).
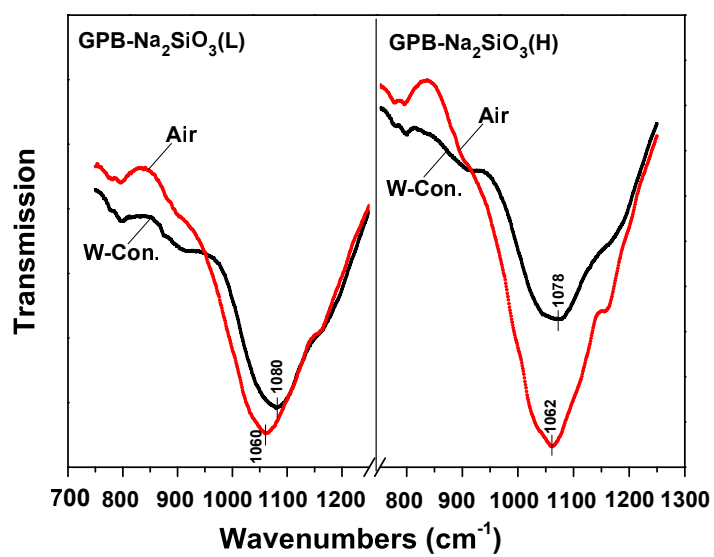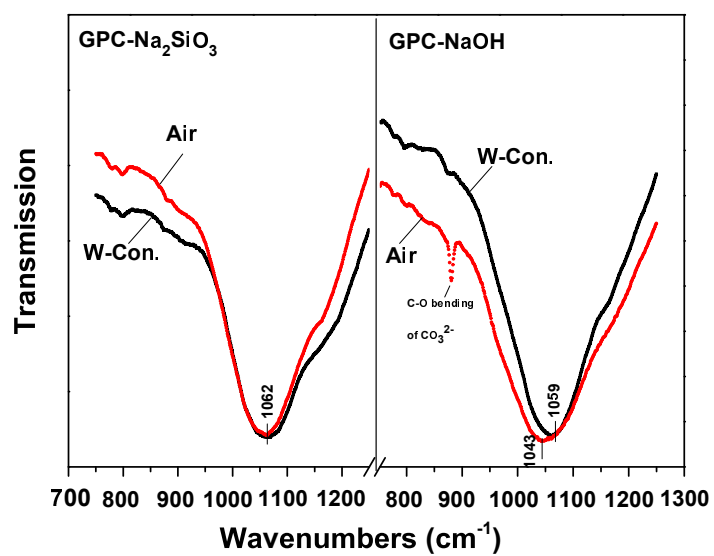
(a)

(b)

Fig.9. SEM images of the efflorescence products: (a) on the surface of 28-day air aged GPC-
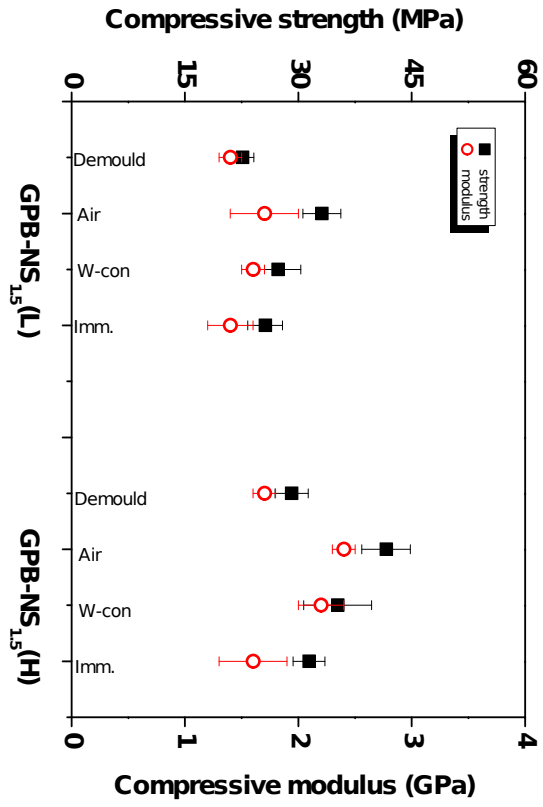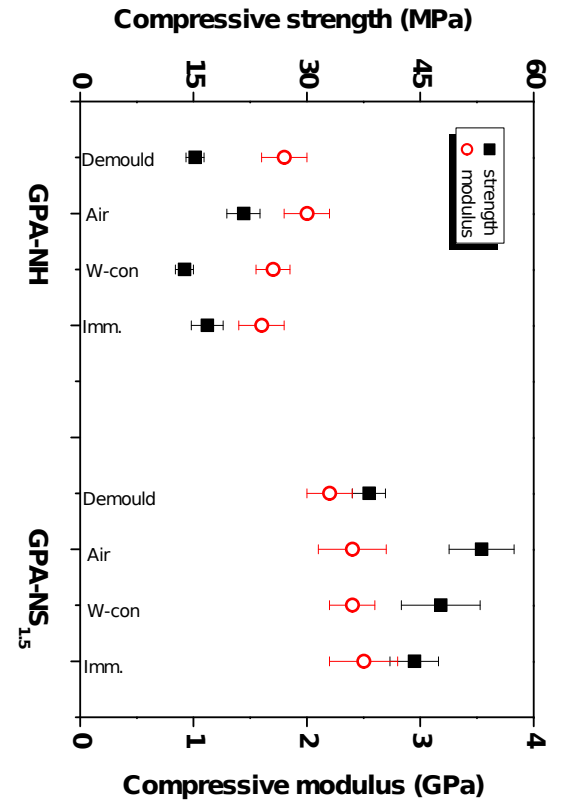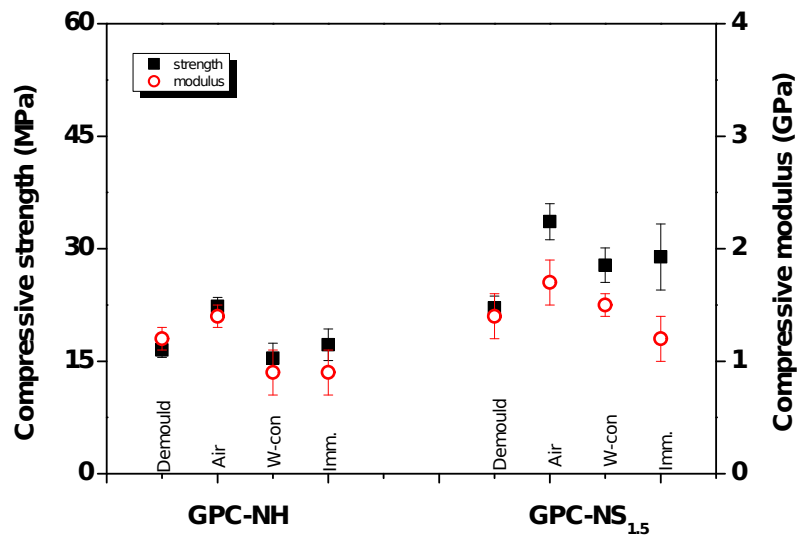NS$_{1.5}$, and (b) the carbonation products on a fracture surface.

Fig. 10. FTIR spectra of geopolymers aged in ambient air and in contact with water at bottom: (a) GPB; (b) GPC.

(a)

(b)

(c)

Fig. 11. Compressive strengths and modulus of the hardened geopolymers on demoulding, and after 28 days of ageing under the three conditions: (a) GPA, (b) GPB and (c) GPC.

Fig.12. (a) Deterioration of foamed geopolymer FGPA after 7 days in contact with water at the bottom; (b) Deterioration of low temperature cured geopolymer LGPC after 90 days of exposure to simulated efflorescence conditions with regular addition of water at bottom; (c) Schematic drying of geopolymer in contact with water and the consequent crystallisation, following [36].

Fig.13. FTIR spectra of the efflorescence product on the surface of LGPC, and the subflorescence product grown under the spalling layer.

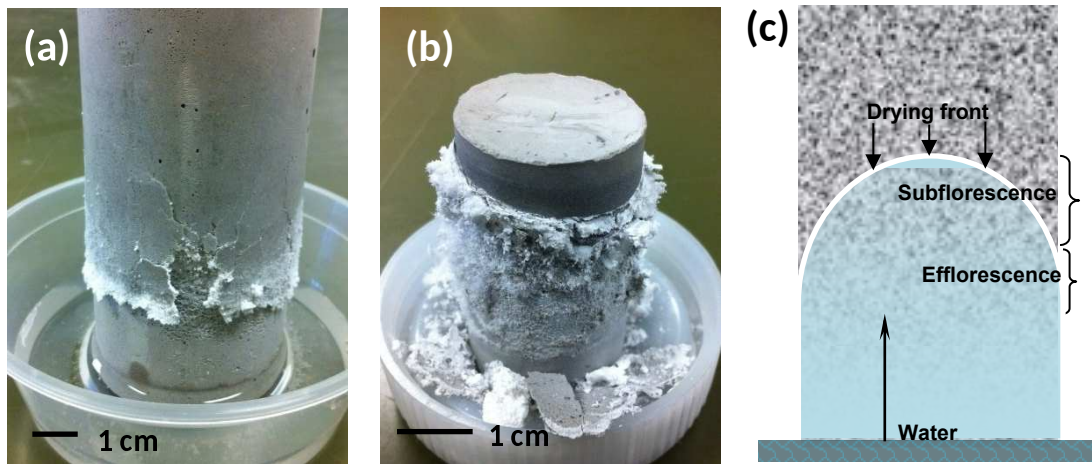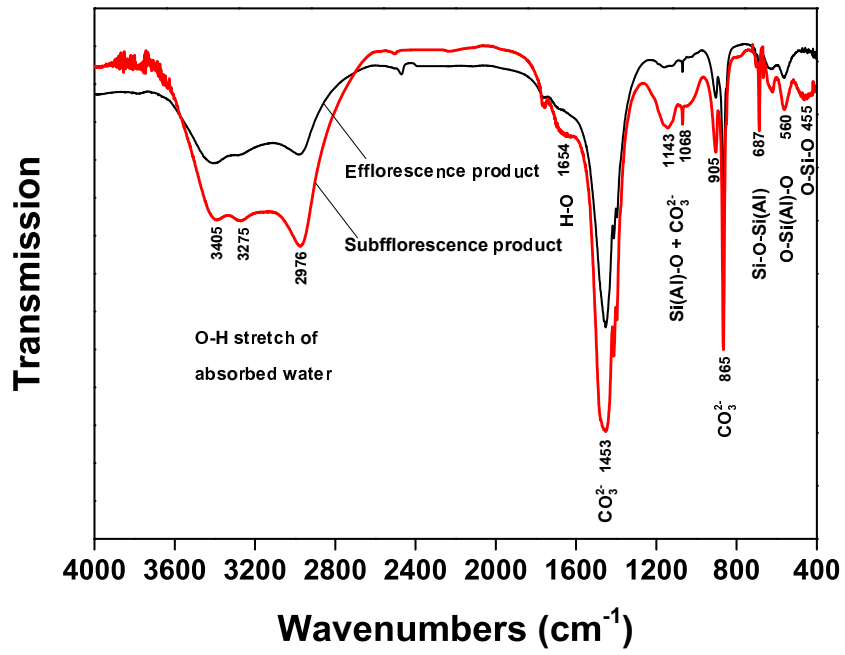| Fig. 1	Particle size distributions of fly ashes A, B and C.
Fig. 2	Particle morphologies as determined by secondary electron imaging in an SEM: (a) fly ash A; (b) fly ash B and (c) fly ash C.
Fig. 3	Efflorescence of hardened geopolymer pastes in contact with water at bottom at a depth around 1 mm.
Fig. 4	Porosities of geopolymer pastes as determined by vacuum saturation method.
Fig. 5	Large and transparent efflorescence products appear on the drying top surface of GPC-NH, after 3 hours in contact with water at bottom.
Fig. 6	The leaching of sodium from fractured geopolymer particles (1.25-1.50 mm) in deionised water at a solid/water ratio of 1:50 at 25°C.
Fig. 7	XRD patterns of each fly ash, and of the hardened geopolymers after 28 days of ageing under conditions of ambient air (Air), in contact with water at bottom (W-Con.) and fully immersed (Imm.). (a-b) GPA: mullite PDF# 79-1457; quartz PDF# 83-0539, hematite PDF# 89-0596; magnetite PDF# 89-0691; hydroxysodalite PDF# 011-0401; (c-d) GPB: mullite PDF# 83-1881, quartz PDF# 85-0795; magnetite PDF#89-3584; and (e-f) GPC: chabazite-Na PDF#019-1178.
Fig. 8	SEM images of geopolymers after ageing in the ambient air (left) and in contact with water at the bottom (right).
Fig. 9	SEM images of the efflorescence products: (a) on the surface of 28-day air aged GPC-NS$_{1.5}$, and (b) the carbonation products on a fracture surface.
Fig. 10	FTIR spectra of geopolymers aged in ambient air and in contact with water at bottom: (a) GPB; (b) GPC.
Fig. 11	Compressive strengths and modulus of the hardened geopolymers on demoulding, and after 28 days of ageing under the three conditions: (a) GPA, (b) GPB and (c) GPC.
Fig. 12	(a) Deterioration of foamed geopolymer FGPA after 7 days in contact with water at the bottom; (b) Deterioration of low temperature cured geopolymer LGPC after 90 days of exposure to simulated efflorescence conditions with regular addition of water at bottom; (c) Schematic drying of geopolymer in contact with water and the consequent crystallisation, following [36].
Fig. 13	FTIR spectra of the efflorescence product on the surface of LGPC, and the subflorescence product grown under the spalling layer.

Table 1. Chemical compositions of fly ashes as measured by XRF, wt.%. LOI is loss of ignition at 1000 °C.

Fly ash	SiO_2	Al_2O_3	CaO	MgO	K_2O	Na_2O	Fe_2O_3	P_2O_5	TiO_2	LOI
A	47.5	27.3	4.25	1.48	0.54	0.74	14.3	0.91	1.47	0.53
B	54.4	32.1	1.06	0.75	0.22	0.14	7.49	0.09	2.14	0.85
C	53.3	32.5	6.90	0.90	0.59	0.27	3.10	0.10	1.60	0.50

Table 2. Mix proportions of geopolymer pastes. The flowability was measured using a steel cylinder with inner diameter of 50 mm and height of 50 mm.

Mix	Fly ash (g)	12 M NaOH (g)	35% $Na_2O·1.5SiO_2$ (g)	Additional water (g)	Na_2O wt.%	Flowing diameter (mm)
GPA-NS$_{1.5}$	1000	0	360	0	4.6	122
GPA-NH	1000	263	0	0	6.2	117
GPB-NS$_{1.5}$(L)	1000	0	300	60	3.9	110
GPB-NS$_{1.5}$(H)	1000	0	360	10	4.6	102
GPC-NS$_{1.5}$	1000	0	270	80	3.5	107
GPC-NH	1000	263	0	70	6.2	110